

LINKING MOBILITY TO MORPHOLOGY

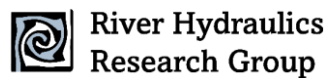
SEDIMENT TRANSPORT CHARACTERISTICS ALONG ALLUVIAL CHANNEL BEDFORMS

6/10/2026

Michael G. Chislett (Presenter)

Bruce J. MacVicar

Frédéric Liébault



West Don River, Toronto

Linking mobility to morphology...

Sediment transport characteristics along alluvial channel bedforms

- In alluvial systems, channelized flow interacts with suspended and bedload sediment
- **Morphology**: the specific shape/form taken by sediment that collects along the channel bed as sequences of units
- **Mobility**: the transport/movement and displacement of sediment with the system

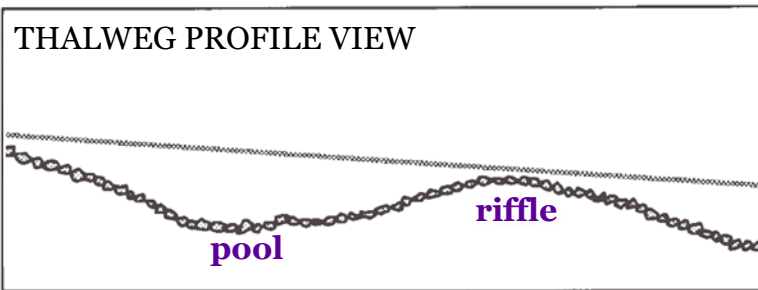
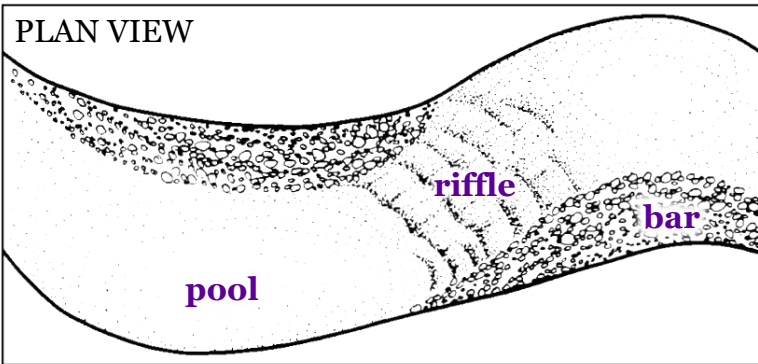
Challenge

We already have lots of **physical definitions** of morphologies, but a single type of morphology can present itself in a **diverse array of local conditions**

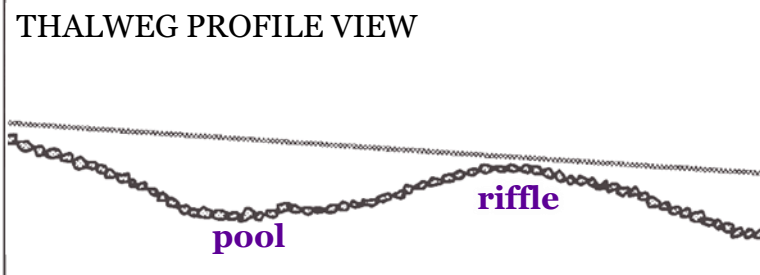
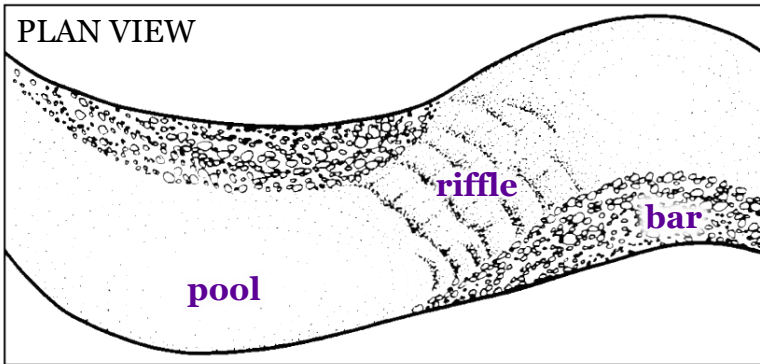
Response

Use **sediment displacement data** to explain the formation criteria of these bedforms, establishing a **framework that helps anticipate** morphology development

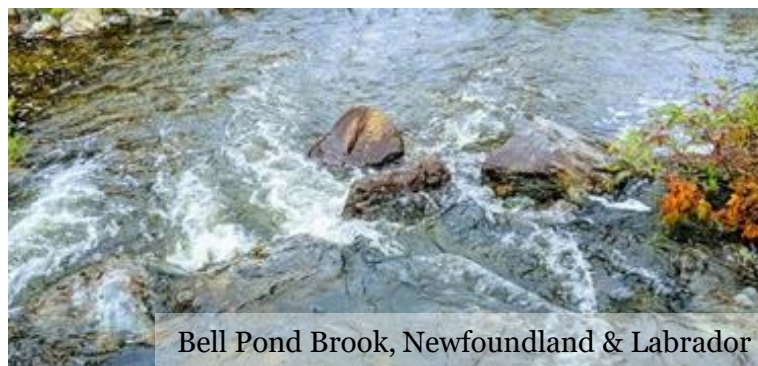
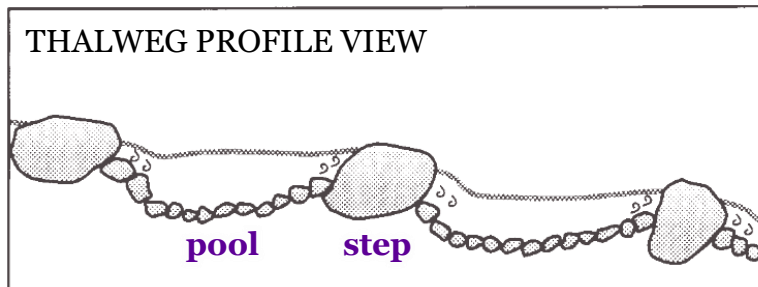
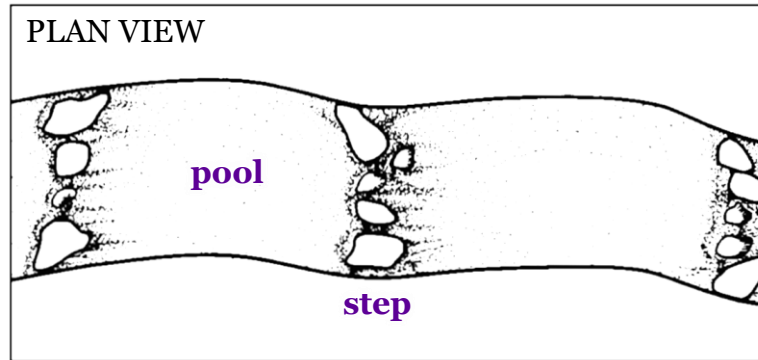
Pool-riffle



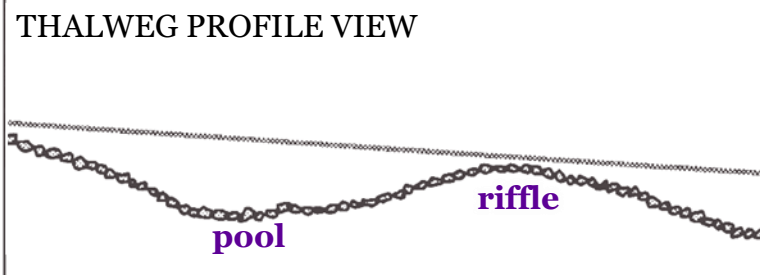
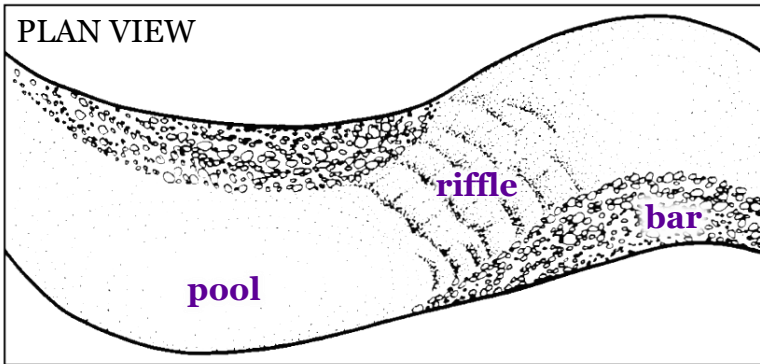
Pool-riffle



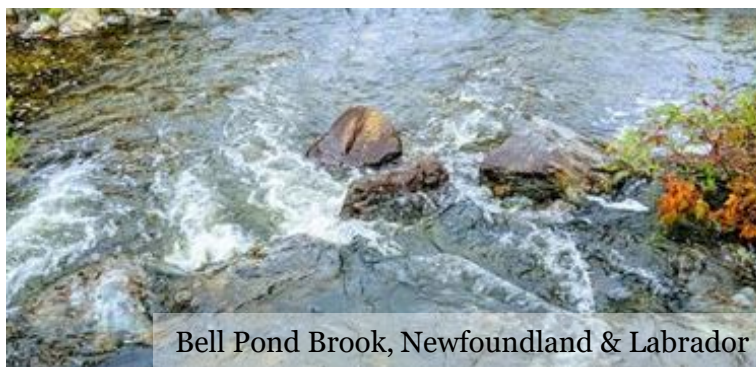
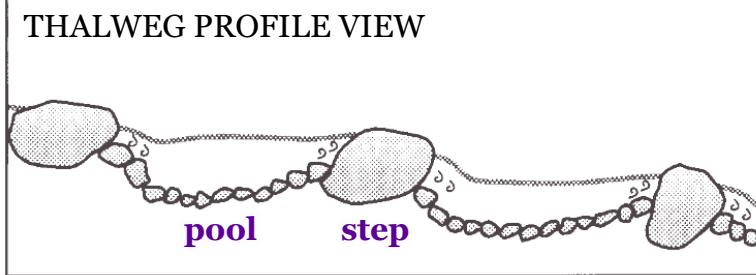
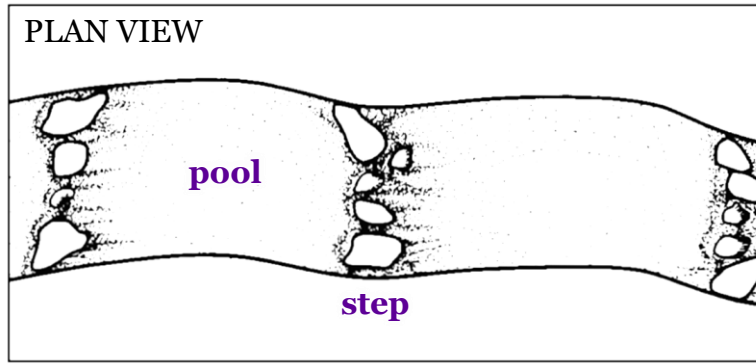
Step-pool



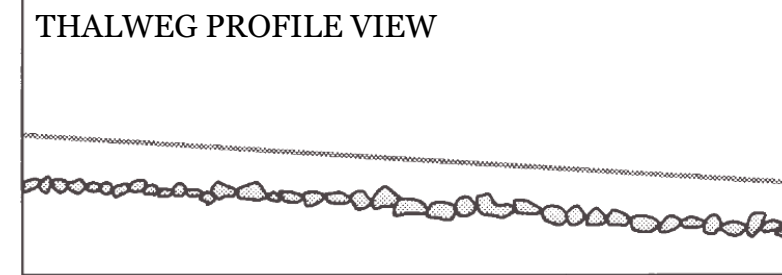
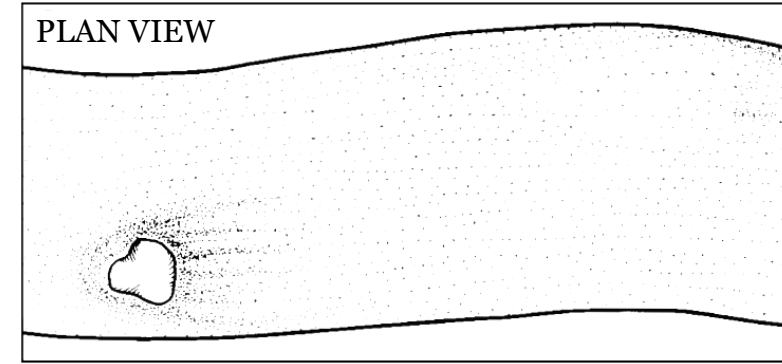
Pool-riffle



Step-pool

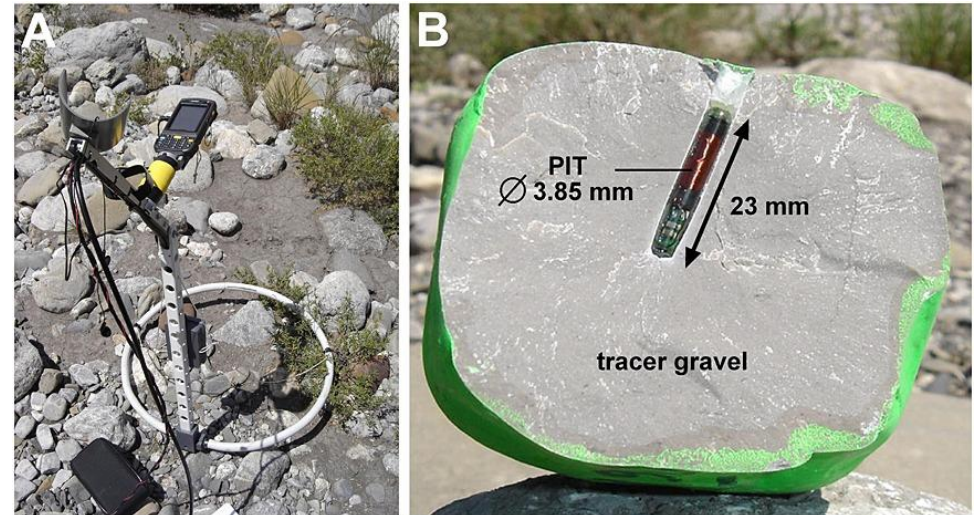


Plane bed



Dataset: Bedload tracing using RFID tags

- Compilation of > 20 years of tracer stone studies by research collaborator Frédéric Liébault (Université Grenoble Alpes) and colleagues
- Measuring bedload sediment transport is a challenge
 - One commonly used method since the early 2000s has been radio frequency identification (RFID) tracer stones
 - A radio antenna (A) is used to detect the location of stones that have been previously implanted and deployed with a passive integrated transponder tag (B). Location of the retrieved stone is then surveyed to acquire a total travel distance



Dataset: Bedload tracing using RFID tags

- Result of the compilation: > 350 RFID surveys + some magnetic tracers, continually being updated whenever new tracer studies are published

	A	B	C	D	E	F	G	H	I	J	K	L	M					
1	RIVER TYPE	REFERENCE	MORPHOTYPE	START	END	DURATION (YR)	N DEPLOY	RECOVERY RATE	MOBILITY RATE	N DIST	MEAN DISTANCE (M)	MEAN DISTANCE D50 (M)	MAX DISTANCE (M)					
2	sand bed river	2004 Nichols					145	0.98										
3	sand bed river	2004 Nichols					195	0.94										
4	boulder bed river	2005 Lamarre et al	plane-bed	2003-09-11	2003-11-27	0.21	204	0.96										
5	boulder bed river	2005 Lamarre et al	plane-bed	2003-11-27	2004-04-28	0.42	204	0.87										
6	gravel bed river	2007 Carré et al	riffle-pool-single-thread	2005-06-21	2005-07-04	0.04	110	0.97					97					
7	gravel bed river	2007 Carré et al	riffle-pool-single-thread	2005-07-04	2005-08-03	0.08	110	0.97					5					
8	gravel bed river	2007 Carré et al	riffle-pool-single-															
9	gravel bed river	2007 Rollet	plane-bed	1	N	O	P	Q	R	S	T	U	V	W	X	Y	Z	AA
				1	WIDTH (M)	SLOPE	D50 (MM)	D84 (MM)	AD (KM2)	QMAX (M3/S)	Qc (M3/S)	OMEGA (W/m2)	exOMEGA (W/m ²)	OMEGA*D50	OMEGA*D84	D/W	D/D50	VIRTUAL VELOCITY (m/yr)
10	gravel bed river	2007 Rollet	riffle-pool-single-	2	n/a	0.0290	n/a	n/a	0.044									
11	boulder bed river	2008a Lamarre and Roy	step-pool	3	n/a	0.0360	n/a	n/a	0.044									
12	boulder bed river	2008a Lamarre and Roy	step-pool	4	7.0	0.0230	70.0	167	14.0	3.50		112.82		0.09	0.03			
13	boulder bed river	2008a Lamarre and Roy	step-pool	5	7.0	0.0230	70.0	167	14.0	3.50		112.82		0.09	0.03			
14	boulder bed river	2008a Lamarre and Roy	step-pool	6	35.0	0.0015	39.0	70	130.0	21.08		8.86		0.02	0.01			
15	boulder bed river	2008a Lamarre and Roy	step-pool	7	35.0	0.0015	39.0	70	130.0	8.00		3.36		0.01	0.00			
16	gravel bed river	2010 Camenen et al	riffle-pool-single-	8	35.0	0.0015	39.0	70	130.0	14.11		5.93		0.01	0.00			
17	gravel bed river	2010 Camenen et al	riffle-pool-single-	9	80.0	0.0014	118.0	126	3670.0	850.00		145.92		0.06	0.05	0.54	364.4	44.5
18	gravel bed river	2010 Camenen et al	riffle-pool-single-	10	90.0	0.0008	46.0	62	3670.0	950.00	325.00	82.84	54.50	0.13	0.08	0.77	1500.0	68.1
19	gravel bed river	2011 Capanni	plane-bed	11	6.0	0.1400	160.0	n/a	3.2	2.04		466.96		0.11		0.64	24.0	8.0
				12	6.0	0.1400	160.0	n/a	3.2	1.20		274.68		0.07		0.26	9.6	4.5
				13	6.0	0.1400	160.0	n/a	3.2	3.40		778.26		0.19		0.84	31.3	3.0
				14	6.0	0.1400	160.0	n/a	3.2	2.11		482.98		0.12		1.39	51.9	24.1
				15	6.0	0.1400	160.0	n/a	3.2	1.36		311.30		0.07		1.38	51.8	12.7
				16	60.0	0.0100	n/a	n/a	1957.0	110.00		179.85				0.10		16.5
				17	60.0	0.0100	n/a	n/a	1957.0	110.00		179.85				0.54		43.2
				18	60.0	0.0100	n/a	n/a	1957.0	130.00		212.55				1.64		125.3
				19	10.0	0.0040	80.0	n/a	186.0	17.00	20.00	66.71		0.05		1.50	187.5	

Mean travel distance, D_{84} , specific stream power

The diversity of pool-riffle morphologies



The diversity of pool-riffle morphologies

Bruce MacVicar^{a,*}, Doug Thompson^b

^a Department of Civil and Environmental Engineering, University of Waterloo, 200 University Avenue West, Waterloo, Ontario N2L 3G1, Canada
^b Department of Physics, Astronomy and Geophysics, Environmental Studies Program, Connecticut College, 270 Mohegan Avenue, New London, CT 06320, USA

ARTICLE INFO

Keywords:
Morphologic classification
Gravel-bed river
Pool riffle
Velocity reversal hypothesis
Flow-convergence routing
Bedforms
Continuum concept

ABSTRACT

Pool-riffle sediment and flow dynamics have been studied for many years, but relatively little work has investigated how variations in flow and sediment regimes might lead to a diversity of pool-riffle morphologies. In this letter we analyze a database of quantitative and qualitative measurements from sites where pool-riffle morphologies have been studied and assess the sites relative to morphologic transitions and mobility thresholds. Results show that pool-riffle sites are stretched over a morphologic gradient of predicted bar types from scrolls to chutes and a modelled mobility gradient from threshold to low transport channels. Flow- and sediment-driven phenomenon that are relevant for pool-riffle mechanics are discussed in this context.

1. Introduction

Many gravel-bed rivers are characterized by an undulating bed morphology, with the deeper areas called pools and the shallower areas called riffles. Pool-riffles can occur in meanders or straight channels (Leopold and Wolman, 1957), and in alluvium or bedrock (Keller and Melhorn, 1978). They can be free-formed or forced by channel obstructions (Keller and Melhorn, 1978; Lisle, 1986), and valley wall irregularities (White et al., 2010). Originally identified visually or on the basis of 1D plots of thalweg elevations (Richards, 1976; O'Neill and Abrahams, 1984; Lisle and Hilton, 1992), the pool-riffle or pool-bar bedform is now understood as a building block of rivers, with different spatial arrangements and scour mechanisms spurring different emergent morphologic types (Thompson, 1986; Ferguson, 1987; Kleinhans and van den Berg, 2011). Modern data acquisition has allowed pools and riffles to be placed within assemblages of geomorphic units (Wyrick and Pasternack, 2014; Wheaton et al., 2015; Pasternack et al., 2018a; Fryirs and Brierley, 2022) that appear within a continuum of macroscale systems where channel patterns are driven by the balance of available energy from the water flow and the work needed to transport the supply of sediment (Lane, 1955; van den Berg, 1995; Church, 2006; Buffington and Montgomery, 2022).

Site investigations of the form and processes of pool-riffles have been carried out over the last several decades (see review by Thompson and MacVicar, 2022), but the diversity of these sites within the continuum of channel form and process has not been examined. Researchers

investigating pool-riffle processes have typically selected study sites without a clear understanding of the diversity of the morphology and associated physical regimes, but the wide range of widths, gradients, sinuosities, and bed materials now provide a basis for describing what is considered a pool-riffle (Thompson and MacVicar, 2022). From the field observations and associated modelling, theories of different mechanisms to explain the formation and maintenance of the form have been advanced, with reviews provided by Milan (2013), Wyrick and Pasternack (2014) and Thompson and MacVicar (2022), among others. In a critique, de Almeida and Rodriguez (2011) note that the “mechanisms seem to operate under specific circumstances and that it is difficult to identify a universal process on the basis of flow variables alone,” and present evidence in the support of sediment-driven mechanisms. However, the range of site morphologies, observations, and hypotheses suggests that, based on the principle of equifinality (Schumm, 1998; Buffington and Montgomery, 2013), pool-riffles may arise through multiple singular or interconnected processes. Possible site diversity may help to explain why researchers have arrived at quite different conclusions about pool-riffle formation and maintenance.

Our goal in this letter is to provide a quantitative framework to differentiate between pool-riffle sites. We analyze a database largely compiled by Thompson and MacVicar (2022) of sites that were used to study pool-riffle form and process. We argue that we may all be right, and use as motivation the parable of people in the dark feeling different parts of an elephant and arguing about what this fantastical beast really looks like. The hope is that the comparison and juxtaposition of sites will

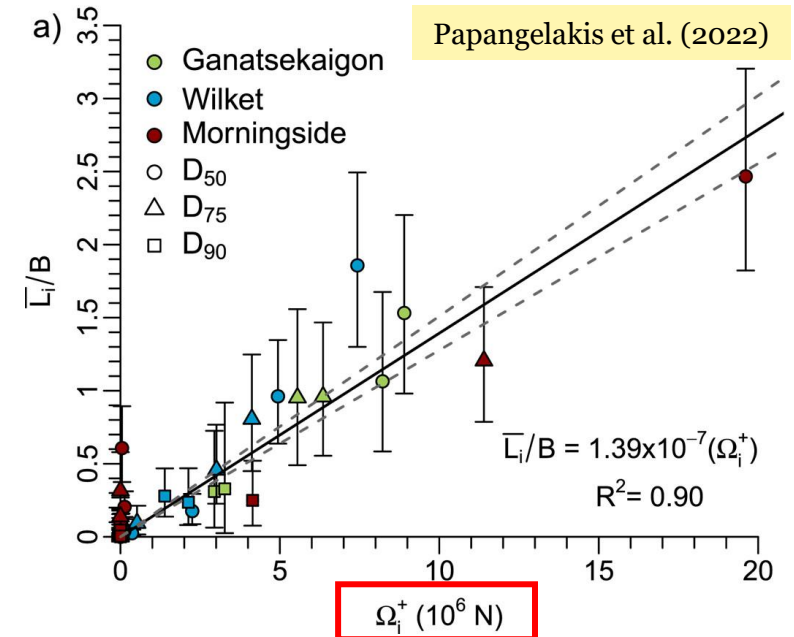
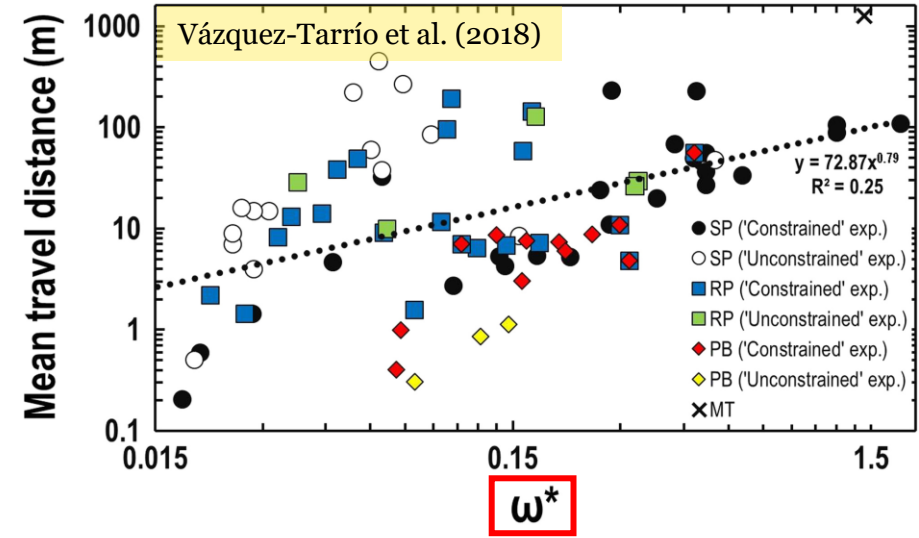
- Goal of the paper: provide a quantitative framework to differentiate between pool-riffle sites.
- Stands as a hypothesis for pool-riffle formation and process that dives deeper into site specific nuances
- Concerned with two channel transition metrics...
 - Mobility thresholds: how different sized sediment moves
 - Morphologic thresholds: how different forms take shape
- This threshold hypothesis is used as the foundation for the updated framework shown in this presentation

Responding to the challenge

- **Hypothesis:** Morphologies will prove statistically different when considered relative to proposed morphologic thresholds
- Different morphologies are expected to experience unique transport behaviours with respect to these new morphologic thresholds
- Past studies have compared transport to the critical mobility stream power, or to the continuous excess stream power

ω^* = dimensionless specific stream power experienced at the peak of an event

Ω_i^+ = cumulative excess total stream power (energy expenditure) over a mobilizing event



Mobility threshold (Ghunowa *et al.*, 2021)

“Does the particle move?”

The critical sediment size at which point entrainment occurs can be estimated from the equations of bed shear stress (τ), the Andrews (1983) hiding function, and Keulegan (1938)’s logarithmic flow resistance equation

Ferguson (2005) put this into the context of a critical D_{84} (the coarse fraction of the bed material)

$$D_{84c} = \frac{1}{\tau_c^* \rho^+ g} \left(\frac{K\omega}{2.3\rho[\log(30\tau_c^* \rho^+) - \log(emS)]} \right)^{2/3}$$

Benefit of this particular derivation: uses channel slope rather than flow depth, which would require local surveying

Morphologic threshold (Kleinhans & van den Berg, 2011)

“What planform pattern do we have?”

van den Berg used a large collection of river data to empirically determine...

$$\omega_m = c_m D_{50}^{0.42}$$

- ω_m = morphologic specific stream power
- c_m = empirical coefficient

$c_m (sc) = 285$	$c_m (bm) = 900$
Meandering channels transitioning from predominantly scroll bars → chute bars	Transition from meandering → braided channels



Morphologic threshold (MacVicar & Thompson, 2023)

$$D_{84m} = 2.2 \left(\frac{\omega}{c_m} \right)^{1/0.42}$$

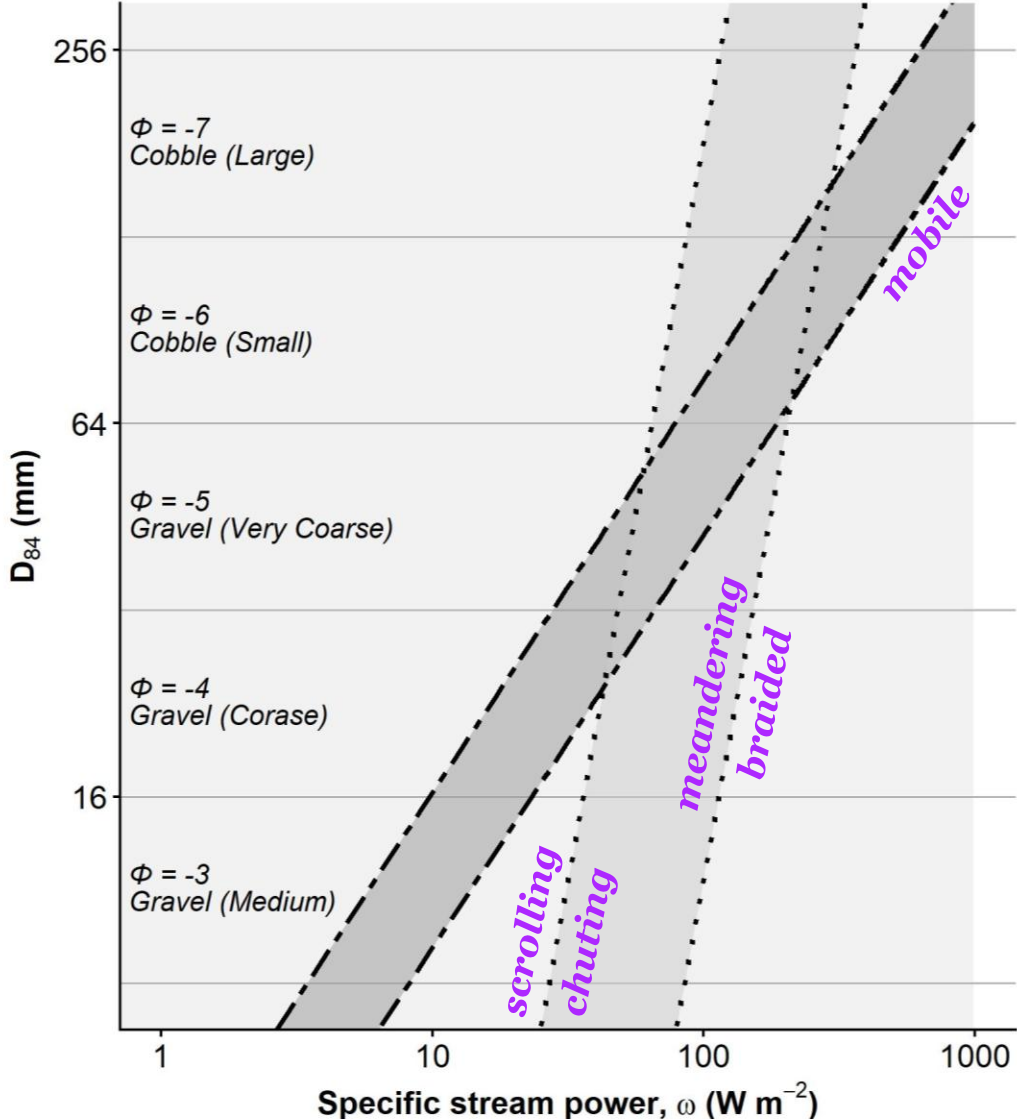
Frames van den Berg in terms of a morphologic D_{84} instead of ω_m by using the López & Barragán roughness height estimation equations

Mobility threshold		Morphologic transitions	
$D_{84c} = \frac{1}{\tau_c^* \rho^+ g} \left(\frac{\kappa \omega}{2.3 \rho [\log(30 \tau_c^* \rho^+) - \log(emS)]} \right)^{2/3}$		$D_{84m} = 2.2 \left(\frac{\omega}{c_m} \right)^{1/0.42}$	
Lower bound: Minimum slope in dataset	Upper bound: Maximum slope in dataset	Lower bound: $c_m = 285$, scrolling to chuting	Upper bound: $c_m = 900$, meandering to braided

Phase diagram

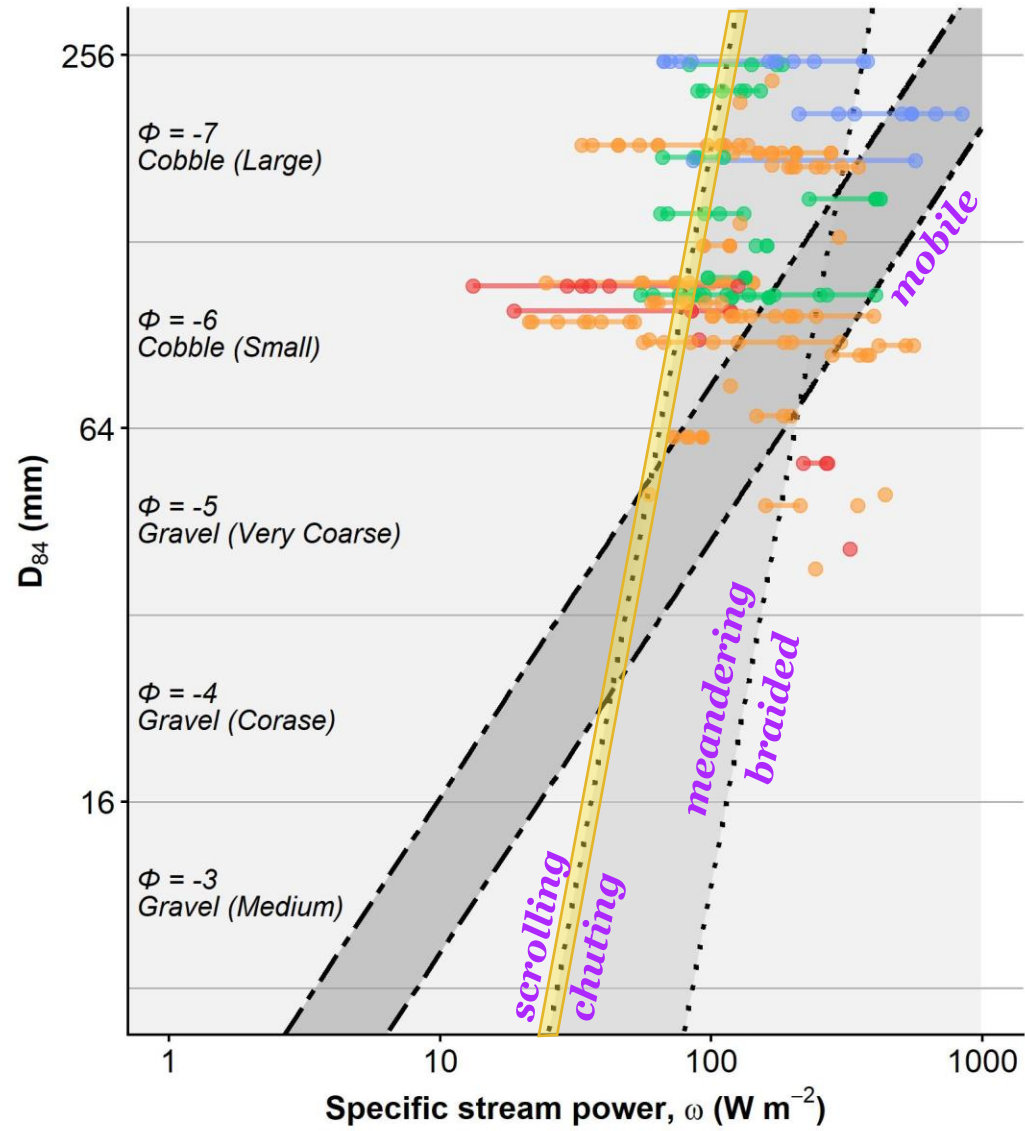
Transition zones

- Mobility transition
- Morphologic transition

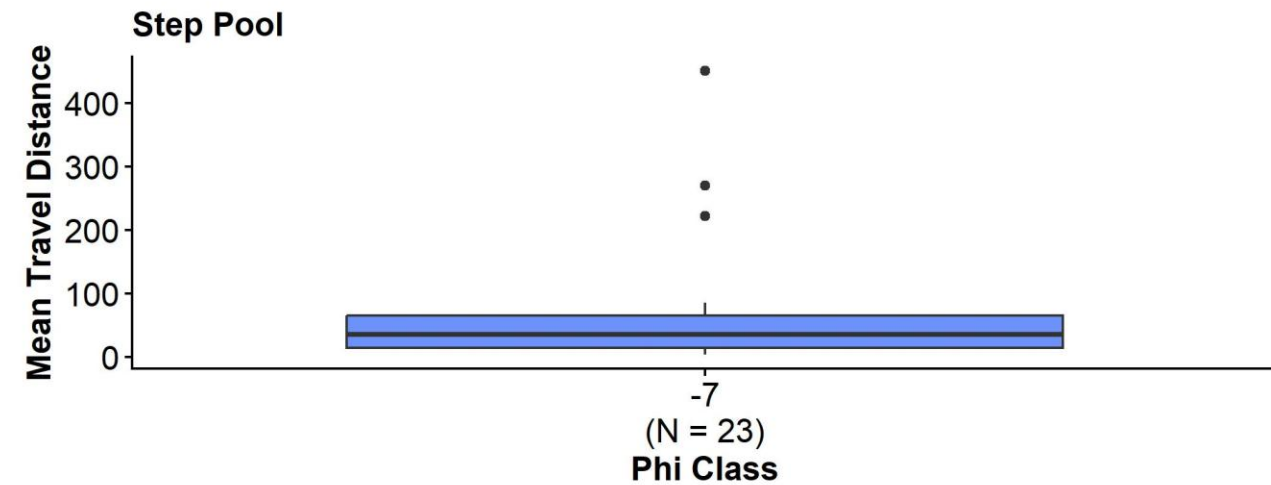
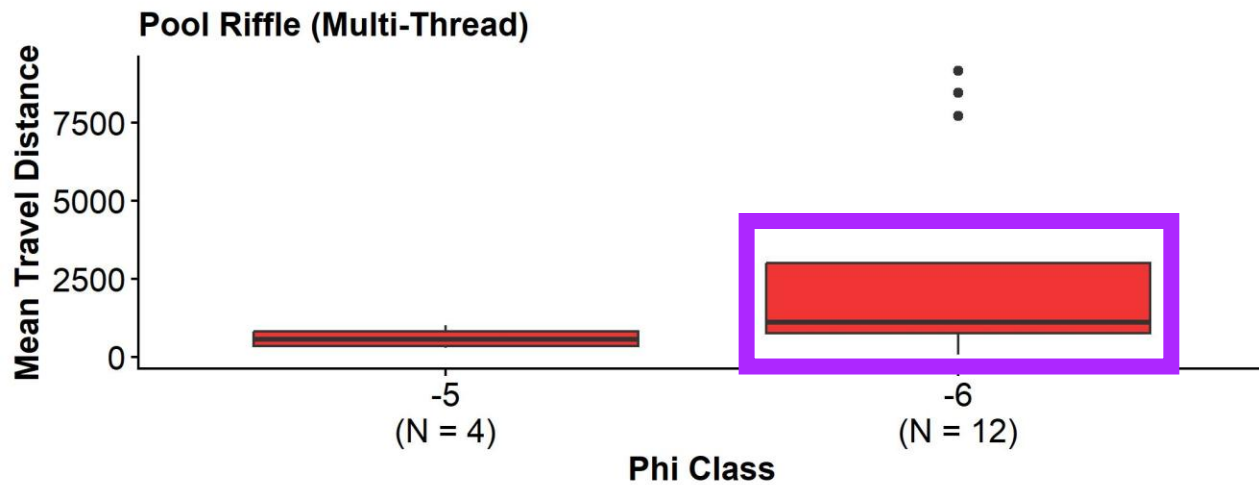
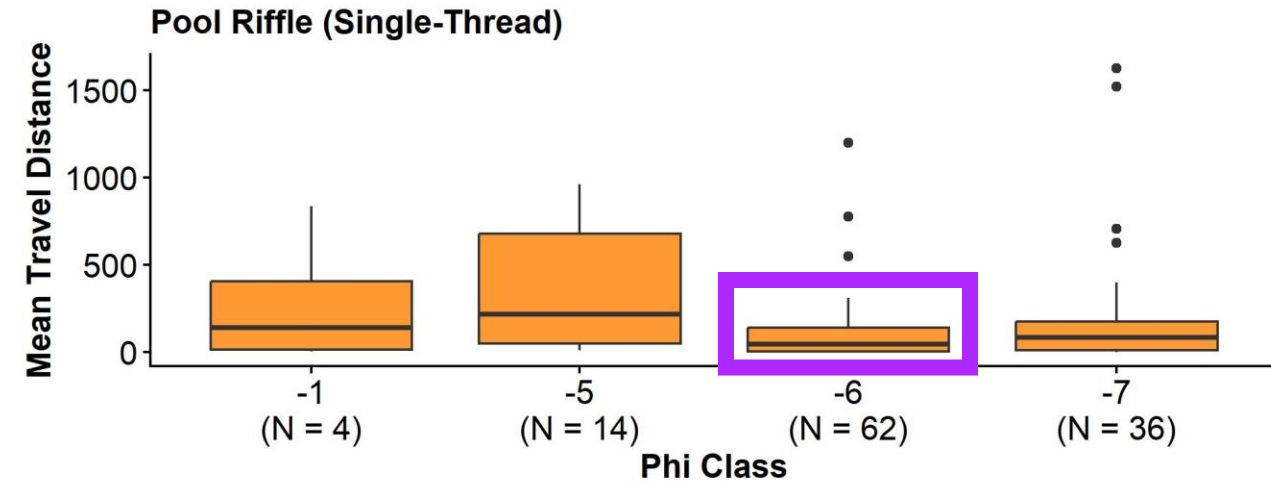
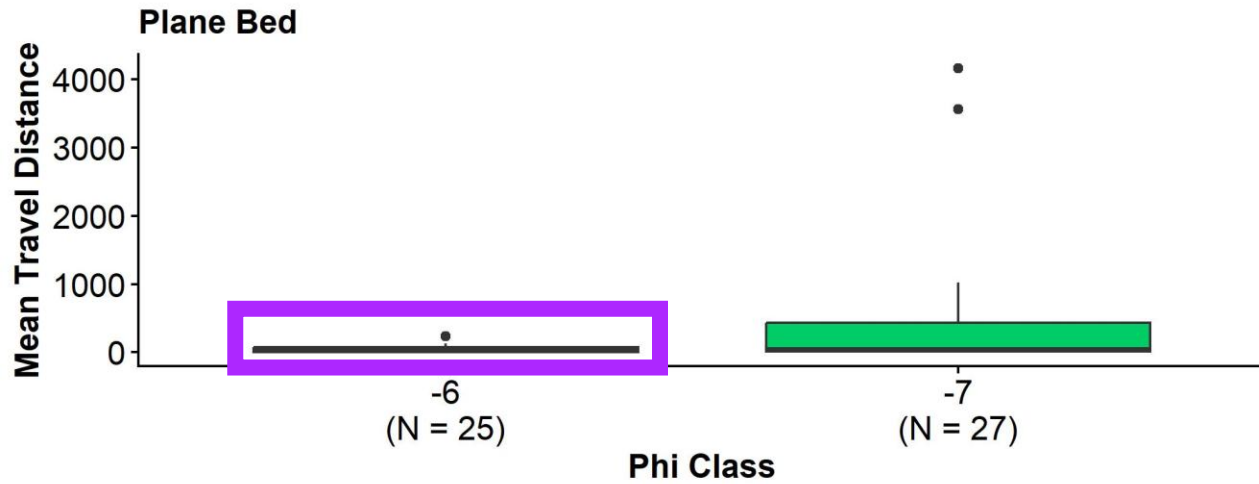


Phase diagram

- Transition zones**
- Mobility transition
 - · Morphologic transition
- Morphotype**
- Pool Riffle (Single-Thread)
 - Pool Riffle (Multi-Thread)
 - Step Pool
 - Plane Bed



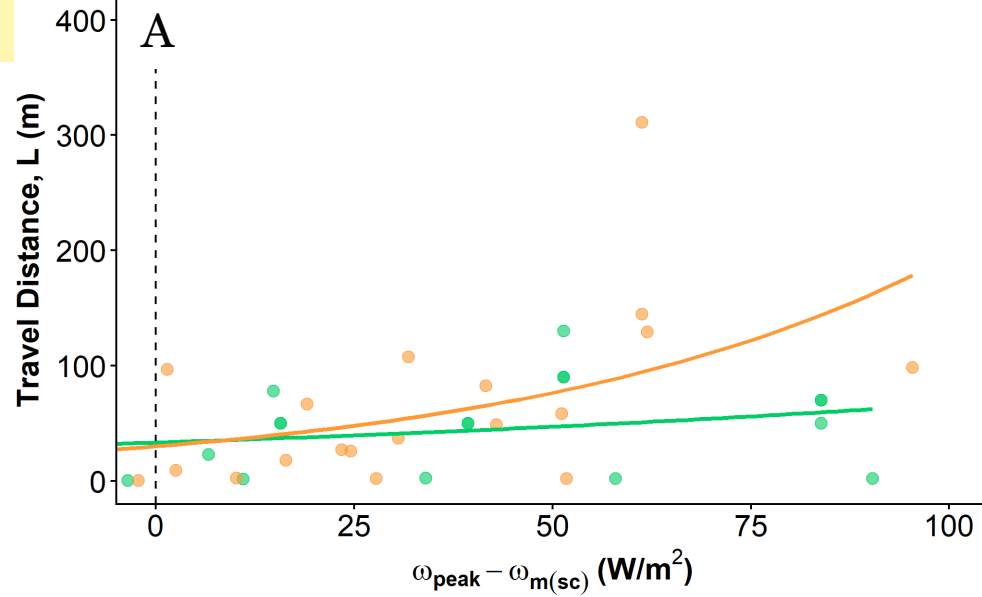
Analysis of outliers



$\Phi = -6$, Cobble (Small)

SPECIFIC Excess Stream Power ($\omega = \Omega/B$)

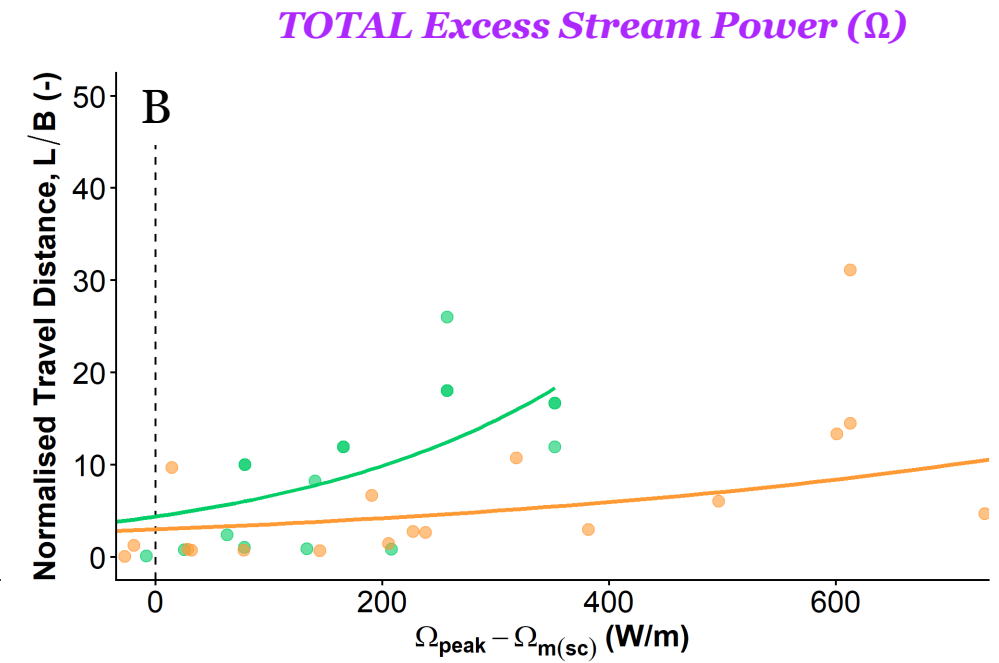
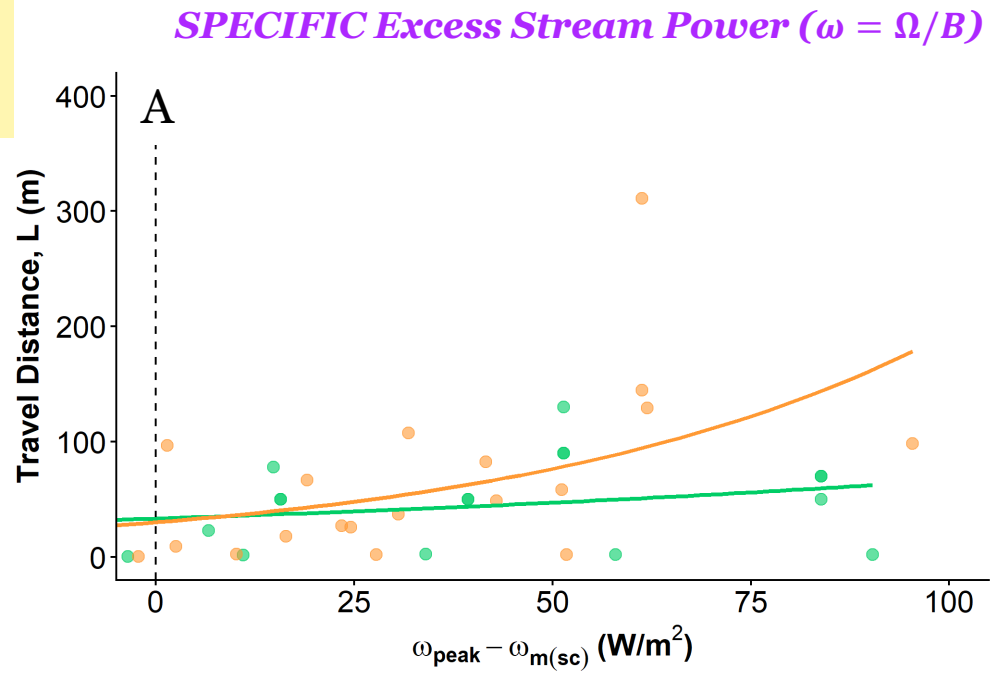
*Morphologic Threshold
(Scrolling \rightarrow Chuting)*



Morphotype ● Plane Bed ● Pool Riffle (Multi-Thread) ● Pool Riffle (Single-Thread)

$\Phi = -6$, Cobble (Small)

*Morphologic Threshold
(Scrolling \rightarrow Chuting)*



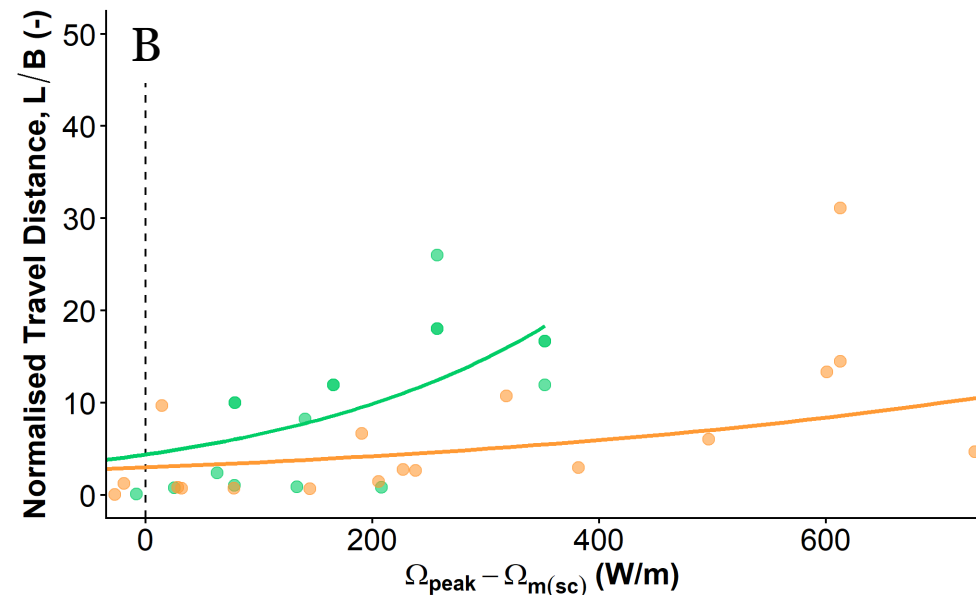
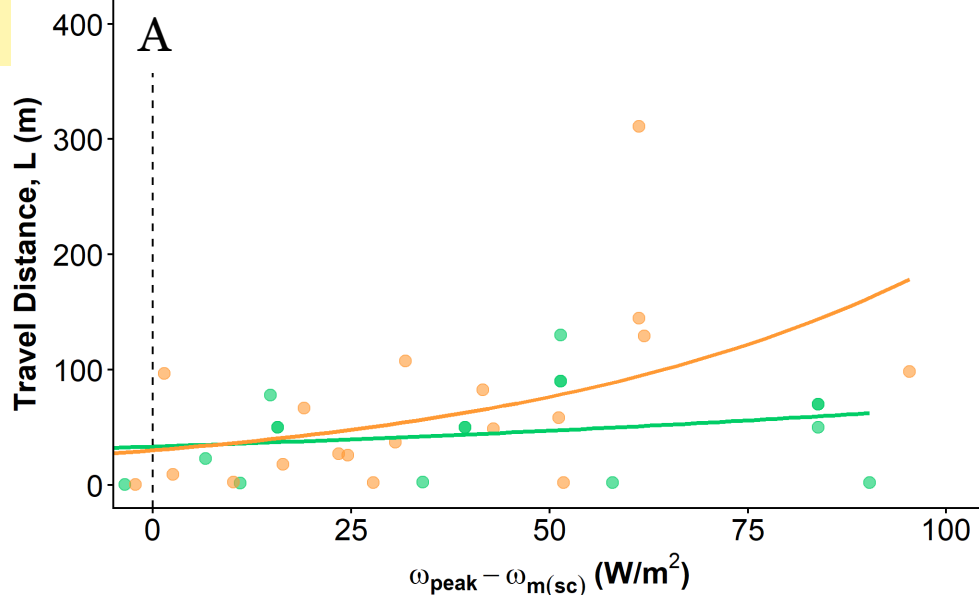
Morphotype ● Plane Bed ● Pool Riffle (Multi-Thread) ● Pool Riffle (Single-Thread)

$\Phi = -6$, Cobble (Small)

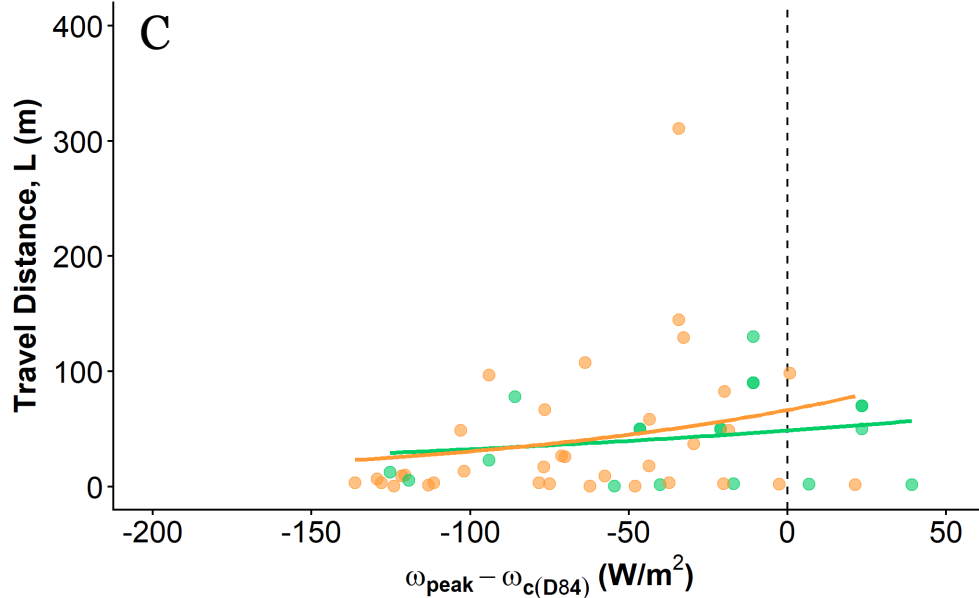
*Morphologic Threshold
(Scrolling \rightarrow Chuting)*

SPECIFIC Excess Stream Power ($\omega = \Omega/B$)

TOTAL Excess Stream Power (Ω)



*Mobility Threshold
(Movement of D_{84})*



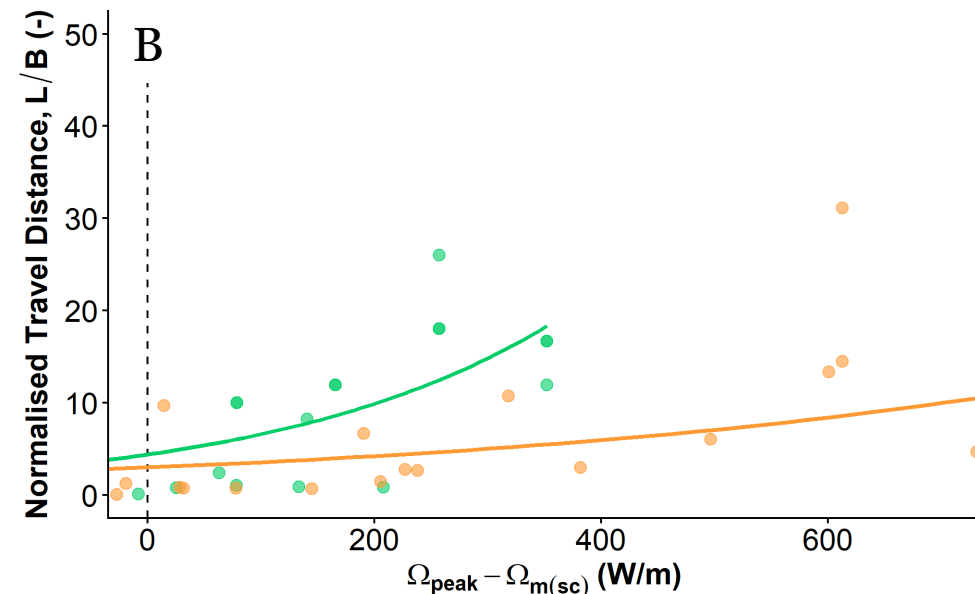
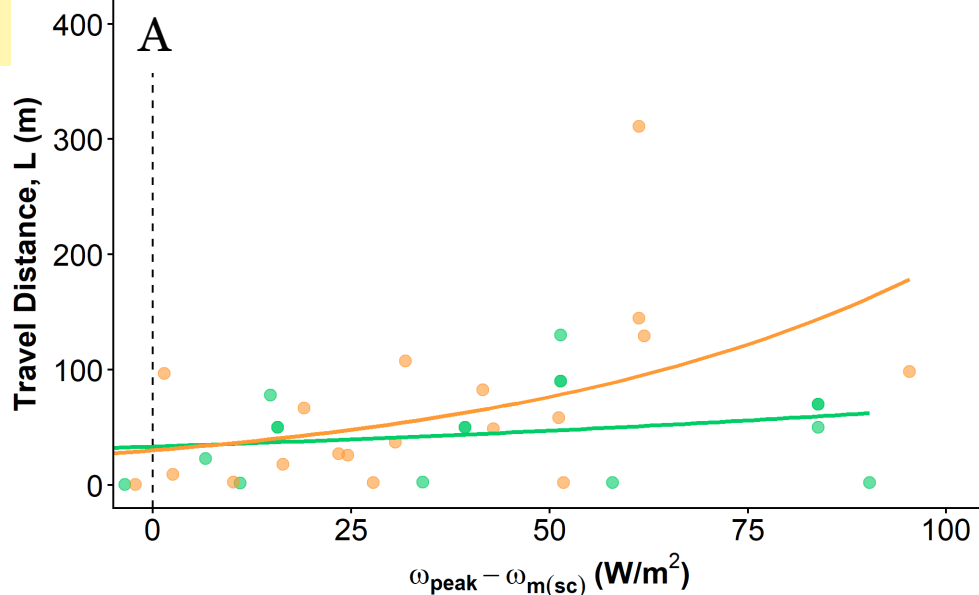
Morphotype ● Plane Bed ● Pool Riffle (Multi-Thread) ● Pool Riffle (Single-Thread)

$\Phi = -6$, Cobble (Small)

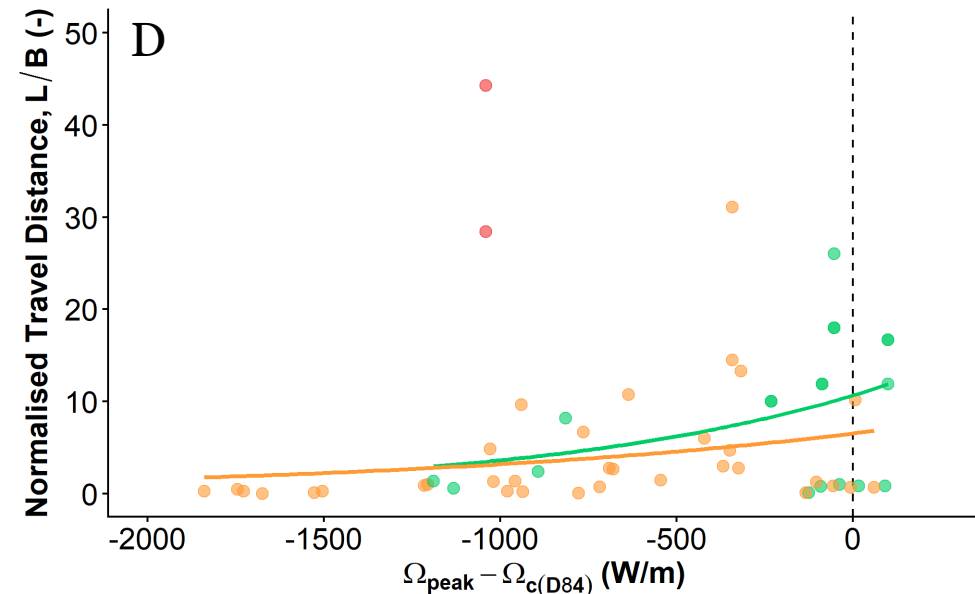
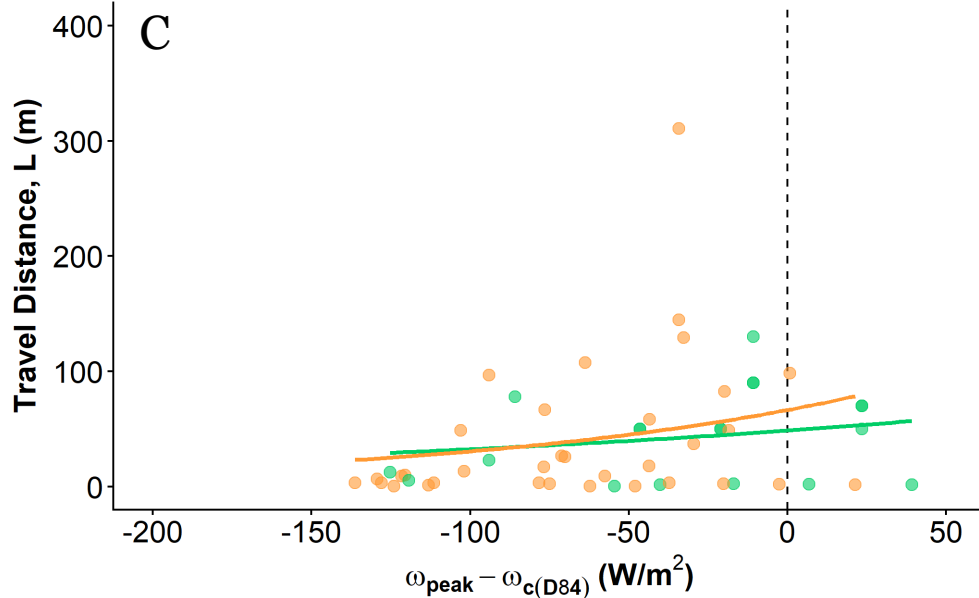
*Morphologic Threshold
(Scrolling \rightarrow Chuting)*

SPECIFIC Excess Stream Power ($\omega = \Omega/B$)

TOTAL Excess Stream Power (Ω)



*Mobility Threshold
(Movement of D_{84})*



Morphotype ● Plane Bed ● Pool Riffle (Multi-Thread) ● Pool Riffle (Single-Thread)

Next steps

- Interpretation of representative grain size critical threshold rather than D_{84}
- Statistical validation
- Upcoming fieldwork:
 - What would additional RFID transport data look like for systems retrofitted with “natural channel designs” in Toronto?
 - What does a “hybrid” (bedload tracing after construction has already been completed) study tell us?

UNIVERSITY OF WATERLOO



FACULTY OF ENGINEERING

Thank you! Merci !

michael.chislett@uwaterloo.ca

Supplementary Material

Mobility threshold (Ghunowa *et al.*, 2021)

$$D_{84c} = \frac{1}{\tau_c^* \rho^+ g} \left(\frac{\kappa \omega}{2.3 \rho [\log(30 \tau_c^* \rho^+) - \log(emS)]} \right)^{2/3}$$

- κ = von Karman coefficient for logarithmic velocity profiles (≈ 0.41)
- $m = 2.8$ = López & Barragán estimation of bed roughness height (empirical multiplier for D_{84})
- ρ^+ = submerged relative density of sediment (≈ 1.6)
- e = Euler's number
- τ_c^* = critical Shields parameter/dimensionless shear stress (≈ 0.045 for D_{50} , used as approximation for D_{84} as well)
- ω = specific stream power = $\frac{\rho g Q S}{B}$
- S = channel slope (Site dependent, but can define a “transitional range” of values from the mildest to steepest slopes in the dataset)

Morphologic threshold (MacVicar & Thompson, 2023)

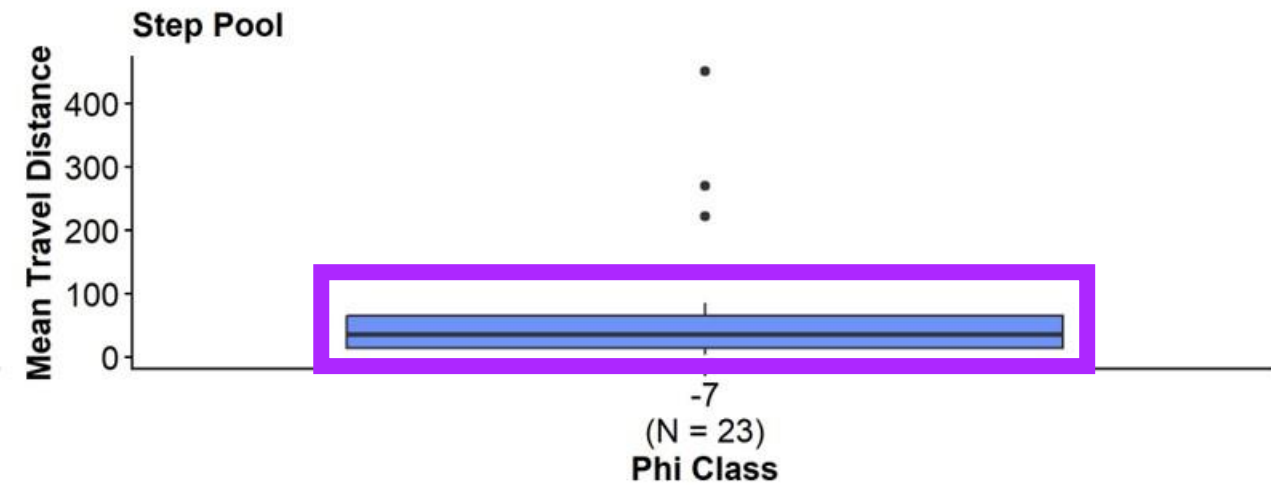
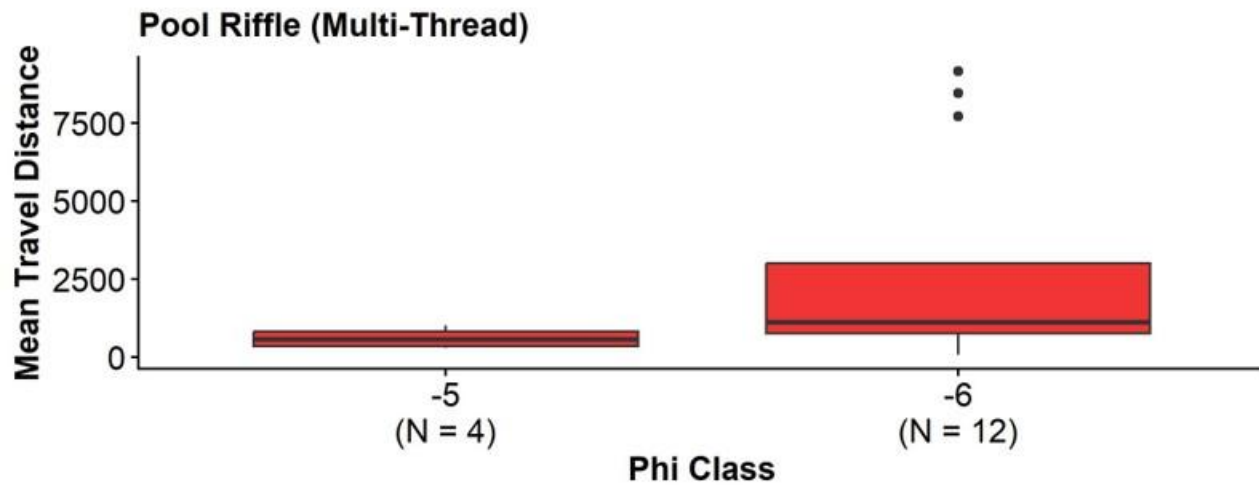
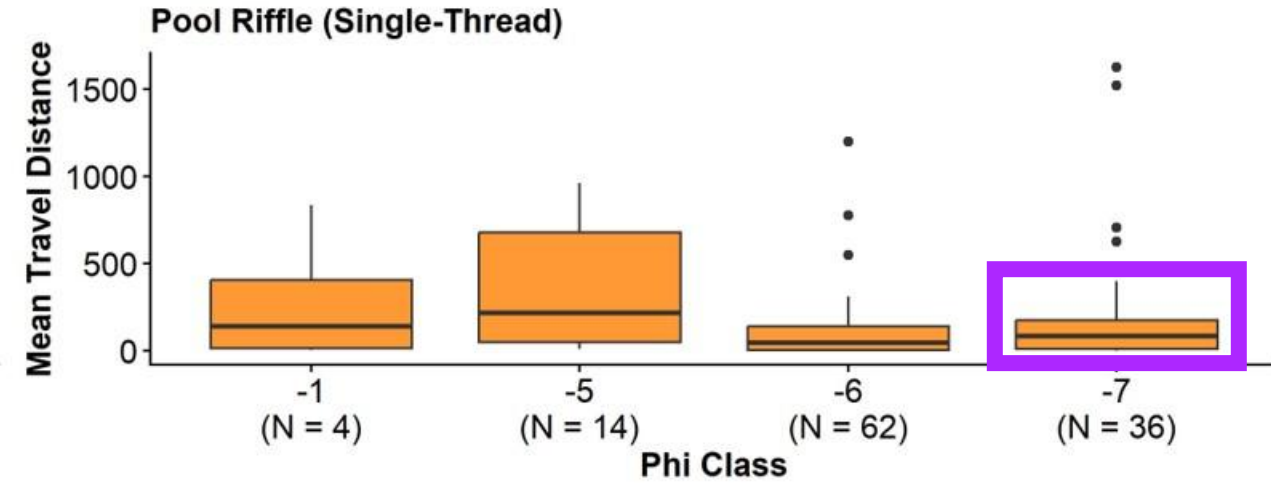
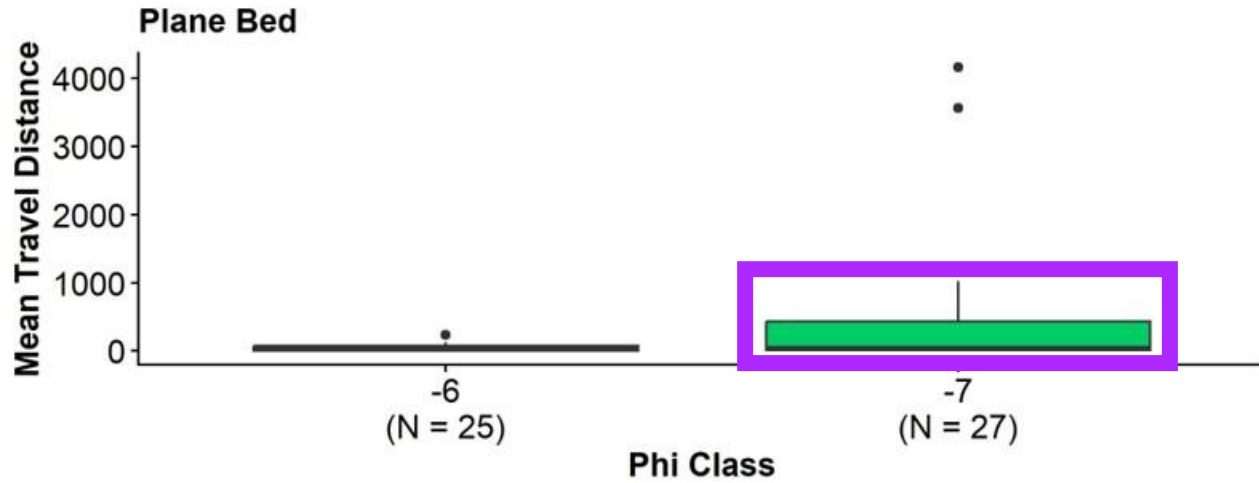
$$D_{84m} = 2.2 \left(\frac{\omega}{c_m} \right)^{1/0.42}$$

Frames van den Berg in terms of a morphologic D_{84} instead of ω_m

Achieved this by using the López & Barragán roughness height estimation equations

- $k_s \approx 2.8D_{84}$ and $k_s \approx 6.1D_{50}$
- So $D_{84} \approx 2.2D_{50}$

Analysis of outliers

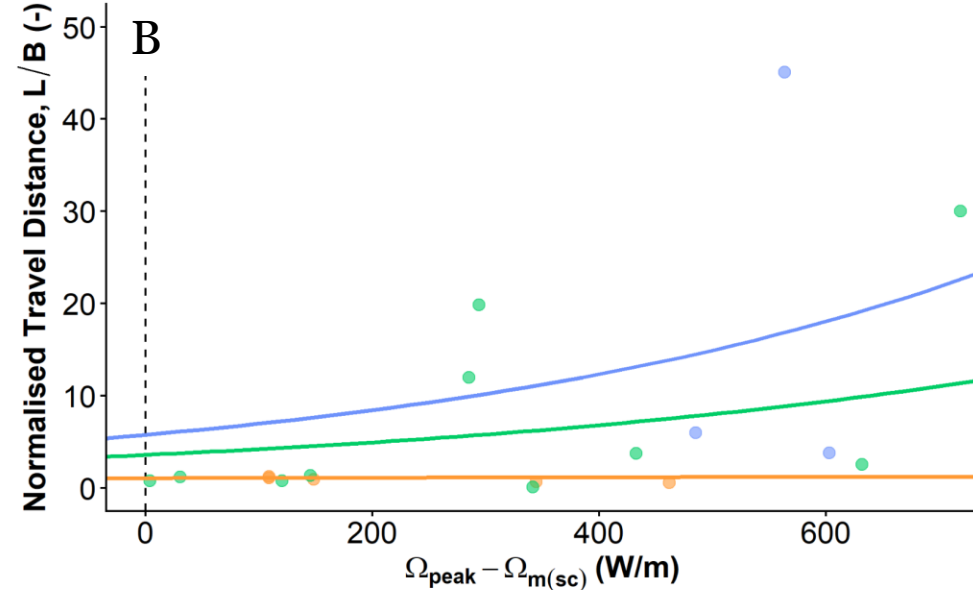
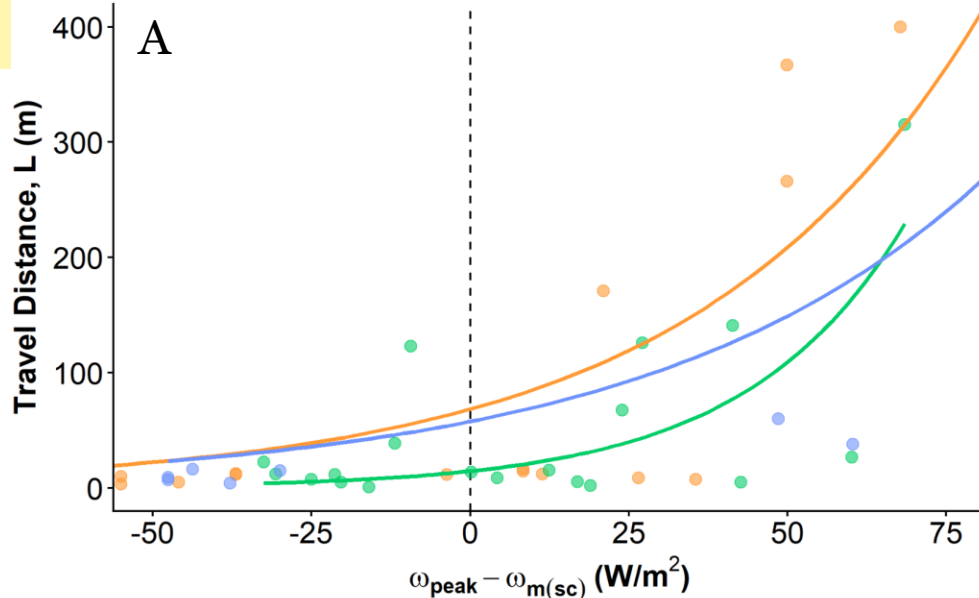


$\Phi = -7$, Cobble (Large)

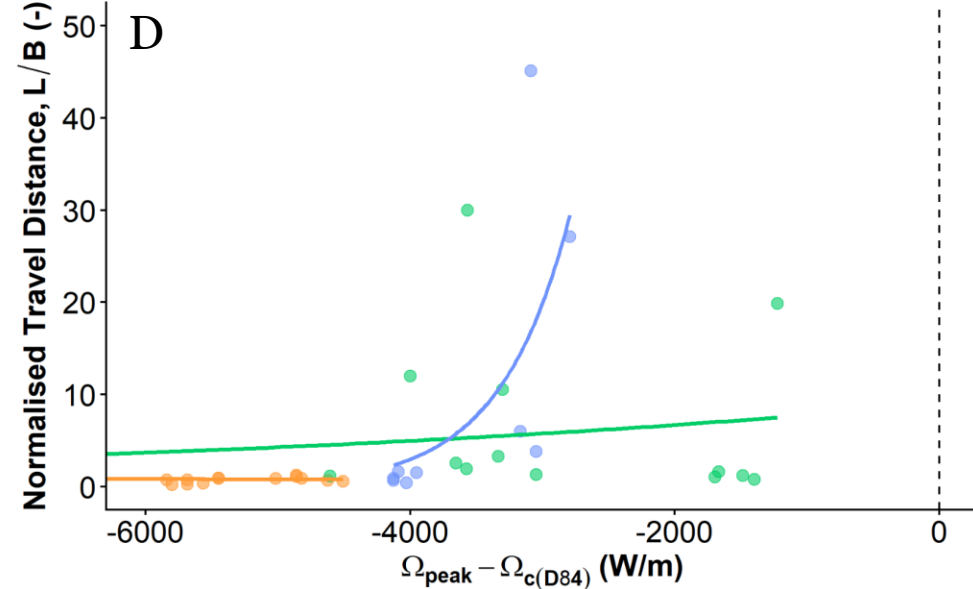
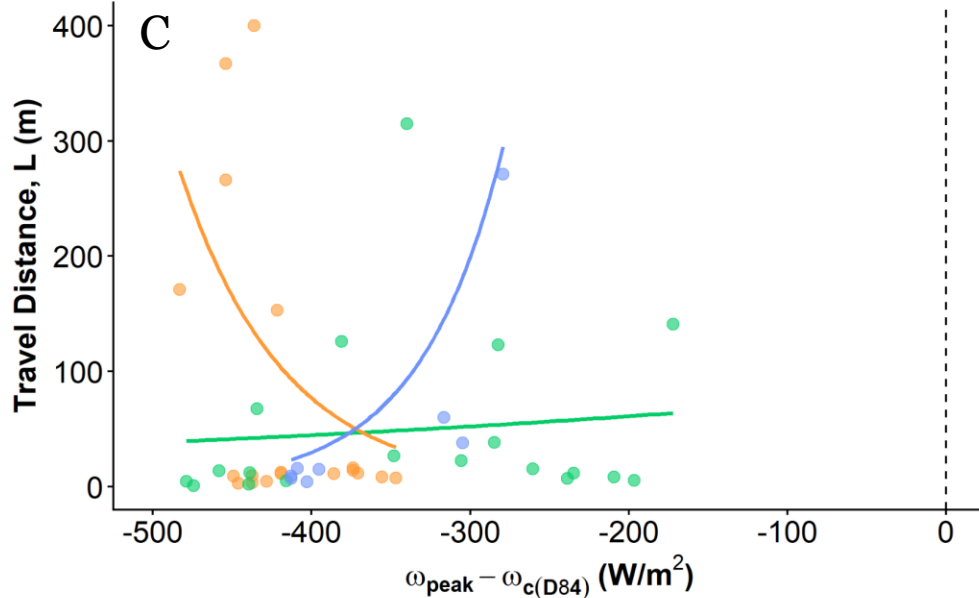
*Morphologic Threshold
(Scrolling \rightarrow Chuting)*

SPECIFIC Excess Stream Power ($\omega = \Omega/B$)

TOTAL Excess Stream Power (Ω)



*Mobility Threshold
(Movement of D_{84})*



Morphotype ● Plane Bed ● Pool Riffle (Single-Thread) ● Step Pool